SAND2014-17731J

Submitted to Particle & Particle Systems Characterization

DOI: 10.1002/ppsc.((please add manuscript number))
Article type: Communication

Self-Assembled Array of Tethered Manganese Oxide Nanoparticles for the Next Generation of Energy Storage

Todd C. Monson, Tyler E. Stevens, Charles J. Pearce, Caleah N. Whitten, Richard P. Grant*

((Optional Dedication))

T. C. Monson, T. E. Stevens,[+] C. J. Pearce, C. N. Whitten,
Sandia National Laboratories, Albuquerque, New Mexico 87185, United States
E-mail: tmonson@sandia.gov

[+] Current address: Department of Chemistry, University of Washington, Seattle, Washington, 98195, United States

Keywords: manganese oxide, self-assembly, pseudocapacitor, tethered, catalysis

Many challenges must be overcome in order to create reliable electrochemical energy storage devices with not only high energy but also high power densities. Gaps exist in both battery and supercapacitor technologies, with neither one satisfying the need for both large power and energy densities in a single device.[1-6] One of the largest limitations in the design of electrodes for existing batteries and electrochemical capacitors today is the use of electrochemically inactive material, such as conductive carbon and binders, which limit the active electrode mass to roughly 70-80%.[7-10] Additional challenges come from electrode degradation as a function of cycle life, poor charge transfer, the inability to fully utilize multiple oxidation states, and the use of electrolytes with a low thermodynamic voltage window (this is the case primarily with supercapacitors that utilize aqueous electrolytes).[1-3, 6] We wished to begin addressing these challenges (and others) in energy storage devices by inventing a process to create a self-assembled array of electrochemically active nanoparticles bound directly to a current collector using extremely short (2 nm or less) conductive tethers. Here, we present work that is a step towards that goal, synthesizing a tethered array of MnO

nanoparticles bound to a gold current collector via short conducting linkages, which achieves 99.9% active material by mass (excluding the current collector).

1. Introduction

Electrochemical energy storage devices are the leading means of storing charge where size and weight are critical.[3, 5-7, 11, 12] Although both batteries and supercapacitors have seen significant improvements in recent years, end users of these devices still require substantial improvements in energy density, power density, and reliability[3, 5, 11]. There are many challenges to achieving increased performance in electrochemical energy storage, several of which were mentioned briefly in the abstract above. With some additional details, the most important issues include additional mass from inactive material providing electron conduction and mechanical stability, the inability to fully utilize multiple oxidation states, and in the case of many supercapacitors, limitation to aqueous electrolytes with a low thermodynamic voltage window[2, 3, 6, 12-15]. In the case of a high percentage of inactive material, as many devices are currently designed, the conductive carbon is necessary for transporting charge to and from poorly conductive active materials and the binder is necessary to hold the electrode structure together.[3, 8, 9, 11, 16, 17] Reliability is also a key metric as devices capable of surviving > 1 M cycles would be extremely beneficial.[6, 18] Another factor that must be considered, yet is sometimes neglected by us as a research community, is the cost of the active electrochemical material relative to the intended application.

Our work cannot unfortunately solve these issues in one fell swoop. However, we believe it does provide one small step towards achieving high reliability, energy density, and power density in a single affordable device. What is presented here is the development of a synthesis route for manganese oxide (MnO_x) nanoparticles tethered to a current collector

using conductive organic linkers of 2 nm or less. Depending on the specific choice of active MnO_x material, this self-assembled structure can be used as an anode for Li-ion batteries (MnO), a cathode for Li-ion and Li metal batteries (MnO_2), an electrode for an oxide supercapacitor (MnO_2), or a catalyst for oxygen reduction in Li-air batteries (MnO_2).[17, 19-41] The many applications of MnO_x gives the synthesis route and nanoparticle structure reported on here a wide breadth of potential applications. In the oxide supercapacitor application, MnO_2 nanoparticles can exhibit pseudocapacitance two of ways: faradaic reactions in aqueous solvents (such as a solution of Na_2SO_4) and "extrinsic" pseudocapacitance through Li^+ intercalation in organic electrolytes at sites located at the surface or near-surface regions.[10, 33, 41-46] When operating in the "extrinsic" pseudocapacitor mode, a nanoparticle MnO_x based device would be able to support rapid charge and discharge times due to the extremely short intercalation distances (5 nm or less), operating much more like a supercapacitor and with increased power densities. There has even been at least one report of MnO_2 in an oxide supercapacitor application where a solvent containing multivalent (in this case Ca^{2+}) ions was used.[47] The ability to use organic electrolytes provides a way to boost the electrochemical window of the device where necessary and boost both the operating voltage and energy density. Nevertheless, in some situations it can be beneficial to have a device that can operate using an aqueous electrolyte and avoid some of the safety and other concerns of operating with organic electrolytes. All of these different options and modes of operation makes a MnO_x based nanoparticle structure extremely versatile in the field of energy storage.

The tethered nanoparticle structure presented here addresses many of the current limitations in electrochemical storage devices. The need for rapid charge and discharge times, leading to enhanced power densities, and the ability to operate with larger voltage windows were partially addressed previously. Additional enhancements to charge transfer time would

be seen from a tethered nanoparticle structure. It is no secret that almost all of the top battery and pseudocapacitor materials, as oxides, are extremely poor conductors.[6, 16, 26, 48, 49] The tethered particle architecture takes a step beyond the addition of conductive carbon by limiting the distance charge must travel through an oxide material and providing short conductive "wires" connected to a current collector to rapidly extract the charge after generation in the active material.[7, 10, 13] The eliminating conductive carbon additives and binders by replacing them with conjugated organic linkers leads to a significant amount of inactive electrode material being eliminated. In fact, when excluding the current collector, a tethered nanoparticle electrode has 99.9% active material by mass as opposed to roughly 70-80% active material (by mass) for more traditionally processed electrodes containing binder and conductive carbon. Nanoparticulate active material also address the limited cycle life in electrochemical electrodes, including those based on MnO_x materials.[3, 19, 21, 26] As discrete and free standing nanoparticles, the active material should be well positioned to accommodate significant strain and size change as cations are (de)intercalated or surface chemistry changes occur. Furthermore, the tethered nanoparticle electrode discussed here is not only a step towards the rational design of oxide supercapacitor electrodes, Li battery electrodes, and Li-air catalysts, but a platform to study behaviors such as charge de(insertion), conversion, and transport in a model system. Many parameters in the tethered nanoparticle electrode can be modified (active material chemistry, structure, size, and morphology; conductive linker chemistry; spacing of active material; etc.) and the effect of those modifications studied.

As discussed above, our choice of active material are the manganese oxides, which in addition to their broad range of potential applications (dependent on the choice of a particular MnO_x phase), are widely regarded as excellent charge storage materials due to the availability of multiple oxidation states and the structural ability to incorporate cations.[34-36, 47] Additionally, manganese oxides are very low in cost, particularly when compared to other

materials often used in oxide supercapacitors (RuO_2) and many Li-ion cathode materials, particularly those rich in cobalt and nickel ($LiCoO_2$ and $Li(NiMnCo)O_2$). For example, although RuO_2 has a very high specific capacitance (~1000 F/g) a RuO_2 based capacitor large enough to power an electric vehicle would cost over $1 million.[5] On the other hand, manganese is the 12th most abundant element found in the earth's crust with Ti and Fe being the only transition metals found in higher quantities.[50]

In this work, our primary goal was to demonstrate the viability of self-assembling an array of tethered nanoparticles so we chose to use MnO since there was a demonstrated and fairly robust synthesis for MnO nanoparticles already in the literature and we saw a reasonable path forward to modifying the surface chemistry of the particles to allow tethering to gold current collector.[51] Optimizing the stoichiometry and phase of the manganese oxide would be the subject of future work. Additionally, the MnO nanoparticle synthesis conditions chosen allowed us to restrict the size of the nanoparticles to 20 nm or less (and therefore limit cation insertion distance to a maximum of 10 nm). Furthermore, the synthesis route chosen can also yield Mn_3O_4 nanoparticles of a similar size simply by excluding water as a reagent.[51] Finally, it has been reported that Mn_3O_4 particles can be converted to MnO_2 via an in situ electrooxidation process.[52] Therefore, the single synthesis route reported here can easily produce an array of MnO, Mn_3O_4, or MnO_2 nanoparticles tethered to a current collector.

2. Synthesis and Characterization of Self-Assembled Electrodes

We started by searching the literature for a high yield and straightforward route to produce manganese oxide nanoparticles with a diameter on the order of 10 nm. Another desire was to find a synthesis that used ligands which we could easily exchange for other

surfactants that would be amenable for forming a linkage with a self-assembled monolayer (SAM). Several syntheses were identified but a few proved to not be reproducible in our laboratory. In the end a communication published by Seo et al. provided a reproducible and straightforward route to synthesize MnO nanoparticles with oleylamine ligands.[51] Control over the size of the nanoparticles was also possible by varying the reaction temperature.

Since the synthesis published by Seo et al. used oleylamine surfactants, we felt it should be straightforward to replace the oleylamine ligands with another amine terminated surfactant with a more reactive end group to form the SAM linkage. We chose 4-bromoaniline since it had a bromine termination attached to a phenyl ring. The conjugated structure of the phenyl group is electrically conducting and would facilitate fast charge transport from the tethered nanoparticles to the current collector. The synthesis of MnO nanoparticles with 4-bromoaniline exchanged for oleylamine proceeded smoothly with only a few small changes, as outlined in the experimental section. Fourier transform infrared spectroscopy (FTIR) data of the MnO nanoparticles, synthesized with 4-bromoaniline are displayed in **Figure 1**. The FTIR spectra of neat 4-bromoaniline is provided as a reference. In additional to a successful nanoparticle synthesis as confirmed via transmission electron microscopy (TEM), the FTIR spectra of the nanoparticles contained absorption peaks associated with the phenyl stretching mode (ν = 1458 cm^{-1}) and CH stretching modes (ν = 1458 cm^{-1}, 2954 , 2920 cm^{-1}, 2850 cm^{-1}), which are strong indications that the 4-bromoaniline was bound to the surface of the MnO nanoparticles. In addition to the FTIR spectra in **Figure 1**, a TEM image of the functionalized MnO nanoparticles is displayed in **Figure 2**. The TEM image confirms that essentially all of the synthesized MnO nanoparticles had a diameter under 20 nm.

The next step in preparing a self-assembled array of tethered nanoparticles was to prepare a SAM on a suitable current collector. The SAM would need to be terminated with

an end group which could react with and form a bond with the bromine terminated 4-bromoaniline molecules serving as surfactants on the nanoparticles. Gold was chosen as the current collector since thiol based SAMs on gold are extremely well characterized, their preparation straightforward, and several studies completed on the electron transport in thiol based molecular junctions.[53-57] Furthermore, there is an extensive array of commercially available thiol terminated molecules with many different end groups. Choosing 4-aminothiophenol gave us a route to form a SAM on a gold current collector with an amine termination, which would react with the bromine end group on the MnO particles via an amination reaction. Once again, the conjugated structure of the phenyl group in 4-aminothiophenol is electron conducting and will facilitate fast charge transport from the tethered nanoparticles to the current collector. The 4-aminothiophenol SAM was prepared using standard routes found in the literature and the growth of the SAM confirmed using FTIR spectroscopy (see **Figure 3**).[56, 57] The FTIR spectra of neat 4-aminothiophenol is provided as a reference. Strong indications of the formation of a 4-aminothiophenol SAM include the presence of the following active IR modes: $\nu(NH_2)$ = 3238 cm^{-1}, ν(CH) = 2931 cm^{-1}, ν_s(SH) = 2549 cm^{-1}, ν(CN) = 1085 cm^{-1}, γ(CH) = 838 cm^{-1}. The presence of the phenyl group stretching mode overlaps with water peaks present in the SAM spectra and due to the weaker absorption signal associated with attenuated total reflectance (ATR) FTIR measurements of the SAM they were not discernable (although we believe them to still be present).

The final step in forming a tethered array of MnO nanoparticles was in making a chemical linkage between the nanoparticle ligands and the SAM. An amination reaction between the bromine termination on the 4-bromoaniline and the 4-aminothiophenol forms a linkage between the particles and the SAM. **Figure 4** shows a schematic of how the SAM on gold and functionalized MnO particles react and form an array of tethered nanoparticles.

When the reaction is complete, a largely conjugated pathway exists between the MnO nanoparticles and the gold current collector. Charge tunneling would still need to occur over very short (~ 2 Å) distances at the particle surface, the secondary amine linkage, and at the interface between the thiol group and the gold surface, although evidence exists showing sufficient electron transport should still occur.[53-55]

Wishing to avoid impurities and wanting to keep costs of a process that could be of interest to industry low, we deliberately avoided the use of catalysts to aid the amination reaction. Nevertheless, it is certainly possible that Pd, Cu, or CsOH based catalysts could make the amination reaction more efficient. We chose to allow the nanoparticles and SAM on gold to react in a solution of DMF over a period of 48 hrs. We did experiment with elevated temperatures (50°C) to make the reaction more efficient but there was evidence that either decomposition of the organic ligands, decomposition of the SAM, and/or undesirable side reactions were occurring. A FTIR spectra of the tethered MnO nanoparticles, with the spectra of the 4-aminothiophenol SAM on gold provided as a reference, is displayed in **Figure 5**. Strong indication of the formation of the linkage between the nanoparticles and the gold substrate is evident in the following active IR modes: $\nu(NH_2)$ = 3359 cm^{-1}, ν(CH) = 2929 cm^{-1}, ν(CN) = 1070 cm^{-1}, γ(CH) = 806 cm^{-1}. The increase in the area under the ν(CN) peak gives additional confidence that secondary amine linkage was made and the number of CN bonds for the system doubled.

Further characterization of the self-assembled array of nanoparticles (and confirmation that our chemistry worked) was provided through high resolution scanning electron microcrope (SEM) imaging of the nanoparticle SAM. A high resolution SEM image of the surface is shown in **Figure 6**. In the SEM image, individual particles bound to the gold surface can be resolved. In some regions, the particles aggregated together into small clumps on the gold surface consisting of roughly 3-15 particles. This is not too surprising given the

high surface area of the nanoparticles and short length (~4 Å) of their ligands, which would not provide very much steric hindrance to particle agglomeration either in solution or on the gold surface. Clustering of individual particles can also be observed in TEM images (see **Figure 2**). Particle stabilization and separation both in solution and on the gold surface can be further optimized through careful choice of ligand molecules with similar functionality and increased chain length. However, the choice of ligand length would need to be balanced with the need for good charge transfer.

3. Conclusion

A self-assembled array of MnO nanoparticles bound directly to a gold current collector using short (~1.5 nm) conducting organic linkers was synthesized and characterized. This array of tethered nanoparticles, and new arrays fabricated in a similar fashion, can have an immediate impact as a new route to fabricate oxide supercapacitor electrodes, Li battery electrodes, and Li-air battery catalysts that can operate in both aqueous and organic electrolytes. Furthermore, tethered nanoparticles are a step towards addressing some of the most difficult challenges facing electrochemical energy storage: achieving high energy and power density in the same device, increasing cycle life through a structure more impervious to degradation, decreasing inactive electrode material, and improving charge transfer.

The self-assembly synthesis approach here is amenable to scaling over areas (coating surfaces from a centimeter to a meter scale or even greater). This single synthesis route reported here can easily produce an array of MnO, Mn_3O_4, or MnO_2 nanoparticles tethered to a current collector through easy modification of the nanoparticle synthesis or post synthesis electrochemical oxidation of the manganese. Additionally, the approach can be modified to accommodate a wide range of metal and metal oxide nanoparticles, organic linking chemistries, and substrates. As a logical next step, we plan on characterizing the

electrochemical response of our tethered MnO nanoparticle array in both aqueous and organic electrolytes and write a follow on publication. We also hope this work will excite other researchers to build upon these results and begin to address key problems in electrochemical energy storage.

Experimental Section

Synthesis of MnO nanoparticles and self-assembled electrode: All chemicals and reagents were purchased from Sigma-Aldrich and used as received. Water used in the synthesis of the MnO nanoparticles was treated by a building wide DI water system and had a measured resistivity of 18.2 MΩ. The MnO nanoparticle synthesis followed the approach as described in the publication by Seo, et al. with a few notable differences. Specifically, the oleylamine surfactant and solvent was replaced with 4-bromoaniline. A manganese(II) acetylacetonate or [$Mn(acac)_2$]:4-bromoaniline:water molar ratio of 1:24:10 (0.9 g Mn(acac), 14.6 g 4-bromoaniline, and 0.630 g water) was used and the synthesis was run at 200 °C for 12 hours. The resulting brown suspension was cooled to room temperature and the particles recovered by centrifugation for 15 min. at 4500 rpm and the supernatant removed. A mixture of 10 mL of ethanol and 20 mL of hexanes was then added to the brown precipitate, which was vortex mixed and sonicated for 15 min. at 50 °C to redisperse the particles. The particles were then pelleted by centrifuging at 4500 rpm for 15 min. and resuspended in hexanes.

4-aminothiophenol monolayers were formed on 1 cm square gold coated silicon wafers (SPI Supplies; West Chester, PA). The substrates were sonicated in ethanol for 20 min. and then cleaned using UV/ozone for an additional 20 minutes just prior to immersion in a 1 mmol solution of 4-aminothiophenol in ethanol for a period of 48 hrs. At the completion of the 48 hr. soak, the SAM coated substrates were removed from the 4-aminothiophenol solution, rinsed with ethanol, and blown dry with nitrogen. In order to form the layer of tethered MnO nanoparticles, a 100 μL solution of MnO particles dispersed in hexanes were

added to 10 mL of dimethylformamide (DMF) and allowed to soak at room temperature for a period of 48 hr. along with the SAM coated gold substrate. After the 48 hr. soak time, the nanoparticle coated substrates were removed from the solution, rinsed with ethanol, and blown dry with nitrogen.

FTIR spectroscopy: Fourier Transform – infrared (FTIR) spectra were obtained with a Bruker IFS 66S FTIR spectrometer (Bruker Optics Inc.; Billerica, MA) in a sample chamber purged with nitrogen gas. MnO nanoparticles were pressed into a KBr pellet with a sample concentration of 2 % (w/w). Reference spectra of neat 4-aminothiophenol and 4-bromoaniline were collected by depositing the liquid samples between two KBr windows. FTIR spectra of the 4-aminothiophenol monolayers and tethered MnO nanoparticles were collected via the reflectance-absorbance FTIR spectroscopy (RAIRS) technique using the Seagull accessory from Harrick Scientific (Pleasantville, NY).

Electron microscopy and analysis: Bright field TEM images were acquired with a JEOL 1200 EX (Tokyo, Japan) using an acceleration voltage of 120 kV. The instrument has a point to point resolution of approximately 9 Å. Images were collected on an Advanced Microscopy Techniques (AMT) XR280L-A 2.8 Mpixel CMOS camera (AMT; Woburn, MA). Samples for TEM analysis were prepared by depositing the nanoparticles onto a holey carbon coated copper TEM grid (Structure Probe, Inc.; West Chester, PA). A 3 μL aliquot of MnO nanoparticles suspended in hexanes was withdrawn from a vial immediately after vigorously vortexing and then added to the surface of the TEM grid. Filter paper placed under the TEM grid was used to aid in wicking away excess solvent and to evenly disperse the nanoparticles across the holey carbon surface.

SEM images were collected using the FEI Magellan 400 Extreme High Resolution (XHR) SEM. Images displayed in the publication were taken at a 1.6 mm Working Distance with a 500V/3.1 pA beam in Beam Deceleration (BD) mode after an in situ 2 minute plasma

clean of the sample. In this BD mode, a primary beam energy of 1kV was emitted from the Field Emitter gun and combined with a beam deceleration of 500 V at the sample, which yielded a 500 V beam on the sample surface. This low energy beam voltage provided high resolution imaging with high surface sensitivity, minimizing sample interference without sacrificing resolution and contrast.

All plots were generated using Igor Pro software (WaveMetrics, Inc.; Lake Oswego, OR, USA).

Acknowledgements
T.C.M. would like to thank Jean Leger and Aaron Beavers for their assistance with nanoparticle and tethered array synthesis. This work was supported by the Division of Materials Sciences and Engineering, Office of Basic Energy Sciences, United States Department of Energy. Sandia National Laboratories is a multi-program laboratory managed and operated by Sandia Corporation, a wholly owned subsidiary of Lockheed Martin Corporation, for the U.S. Department of Energy's National Nuclear Security Administration under contract DE-AC04-94AL85000.

Received: ((will be filled in by the editorial staff))
Revised: ((will be filled in by the editorial staff))
Published online: ((will be filled in by the editorial staff))

[1] A. Du Pasquier, I. Plitz, J. Gural, F. Badway, G. G. Amatucci, *J. Power Sources* **2004**, 136, 160.

[2] G. G. Amatucci, F. Badway, A. Du Pasquier, T. Zheng, *J. Electrochem. Soc.* **2001**, 148, A930.

[3] in *Report of the Basic Energy Sciences Workshop on Electrical Energy Storage*, Office of Basic Energy Sciences, Department of Energy, 2007.

[4] P. G. Bruce, B. Scrosati, J.-M. Tarascon, *Angew. Chem. Int. Ed.* **2008**, 47, 2930.

[5] J. R. Miller, P. Simon, *Science* **2008**, 321, 651.

[6] P. Simon, Y. Gogotsi, *Nat Mater* **2008**, 7, 845.

[7] J. M. Tarascon, *Philosophical Transactions of the Royal Society A: Mathematical, Physical and Engineering Sciences* **2010**, 368, 3227.

[8] A. Patil, V. Patil, D. W. Shin, J.-W. Choi, D.-S. Paik, S.-J. Yoon, *Mater. Res. Bull.* **2008**, 43, 1913.

[9] M. Min, K. Machida, J. H. Jang, K. Naoi, *J. Electrochem. Soc.* **2006**, 153, A334.

[10] A. S. Arico, P. Bruce, B. Scrosati, J.-M. Tarascon, W. van Schalkwijk, *Nat Mater* **2005**, 4, 366.

[11] M. S. Whittingham, *MRS Bull.* **2008**, 33, 411.

[12] H. D. Abruna, Y. Kiya, J. C. Henderson, *Physics Today* **2008**, 61, 43.

[13] M. Armand, J. M. Tarascon, *Nature* **2008**, 451, 652.

[14] J. Muldoon, C. B. Bucur, A. G. Oliver, T. Sugimoto, M. Matsui, H. S. Kim, G. D. Allred, J. Zajicek, Y. Kotani, *Energy & Environmental Science* **2012**, 5, 5941.

[15] W. Wang, B. Jiang, W. Xiong, H. Sun, Z. Lin, L. Hu, J. Tu, J. Hou, H. Zhu, S. Jiao, *Sci. Rep.* **2013**, 3.

[16] H. Zhang, X. Yu, P. V. Braun, *Nat Nano* **2011**, 6, 277.

[17] D. Belanger, T. Brousse, J. W. Long, *Electrochem. Soc. Interface* **2008**, 17, 49.

[18] J. R. Miller, A. F. Burke, *Electrochem. Soc. Interface* **2008**, 17, 53.

[19] W. Luo, X. Hu, Y. Sun, Y. Huang, *ACS Applied Materials & Interfaces* **2013**, 5, 1997.

[20] X. Fang, X. Lu, X. Guo, Y. Mao, Y.-S. Hu, J. Wang, Z. Wang, F. Wu, H. Liu, L. Chen, *Electrochem. Commun.* **2010**, 12, 1520.

[21] B. Liu, X. Hu, H. Xu, W. Luo, Y. Sun, Y. Huang, *Sci. Rep.* **2014**, 4.

[22] X. Li, D. Li, L. Qiao, X. Wang, X. Sun, P. Wang, D. He, *J. Mater. Chem.* **2012**, 22, 9189.

[23] K. Zhong, B. Zhang, S. Luo, W. Wen, H. Li, X. Huang, L. Chen, *J. Power Sources* **2011**, 196, 6802.

[24] T. Wang, Z. Peng, Y. Wang, J. Tang, G. Zheng, *Sci. Rep.* **2013**, 3.

[25] K. Zhong, X. Xia, B. Zhang, H. Li, Z. Wang, L. Chen, *J. Power Sources* **2010**, 195, 3300.

[26] B. Sun, Z. Chen, H.-S. Kim, H. Ahn, G. Wang, *J. Power Sources* **2011**, 196, 3346.

[27] S.-Y. Liu, J. Xie, Y.-X. Zheng, G.-S. Cao, T.-J. Zhu, X.-B. Zhao, *Electrochim. Acta* **2012**, 66, 271.

[28] X. Q. Yu, Y. He, J. P. Sun, K. Tang, H. Li, L. Q. Chen, X. J. Huang, *Electrochem. Commun.* **2009**, 11, 791.

[29] W. Si, C. Yan, Y. Chen, S. Oswald, L. Han, O. G. Schmidt, *Energy & Environmental Science* **2013**, 6, 3218.

[30] J.-H. Kim, K. H. Lee, L. J. Overzet, G. S. Lee, *Nano Lett.* **2011**, 11, 2611.

[31] M.-S. Wu, P.-C. J. Chiang, J.-T. Lee, J.-C. Lin, *The Journal of Physical Chemistry B* **2005**, 109, 23279.

[32] C. S. Johnson, *J. Power Sources* **2007**, 165, 559.

[33] C. Xu, F. Kang, B. Li, H. Du, *J. Mater. Res.* **2010**, 25, 1421.

[34] W. Wei, X. Cui, W. Chen, D. G. Ivey, *Chem. Soc. Rev.* **2011**, 40, 1697.

[35] M. M. Thackeray, *Prog. Solid State Chem.* **1997**, 25, 1.

[36] M. M. Thackeray, M. H. Rossouw, A. de Kock, A. P. de la Harpe, R. J. Gummow, K. Pearce, D. C. Liles, *J. Power Sources* **1993**, 43, 289.

[37] J. Christensen, P. Albertus, R. S. Sanchez-Carrera, T. Lohmann, B. Kozinsky, R. Liedtke, J. Ahmed, A. Kojic, *J. Electrochem. Soc.* **2012**, 159, R1.

[38] A. Debart, A. J. Paterson, J. Bao, P. G. Bruce, *Angewandte Chemie-International Edition* **2008**, 47, 4521.

[39] G. Girishkumar, B. McCloskey, A. C. Luntz, S. Swanson, W. Wilcke, *Journal of Physical Chemistry Letters* **2010**, 1, 2193.

[40] Y.-C. Lu, H. A. Gasteiger, E. Crumlin, R. McGuire, Jr., Y. Shao-Horn, *J. Electrochem. Soc.* **2010**, 157, A1016.

[41] P. Simon, Y. Gogotsi, B. Dunn, *Science* **2014**, 343, 1210.

[42] B. E. Conway, *J. Electrochem. Soc.* **1991**, 138, 1539.

[43] B. E. Conway, *Electrochemical Supercapacitors: Scientific Fundamentals and Technological Applications*, Springer, New York **1999**.

[44] V. Augustyn, J. Come, M. A. Lowe, J. W. Kim, P.-L. Taberna, S. H. Tolbert, H. D. Abruña, P. Simon, B. Dunn, *Nat Mater* **2013**, 12, 518.

[45] M. Okubo, E. Hosono, J. Kim, M. Enomoto, N. Kojima, T. Kudo, H. Zhou, I. Honma, *J. Am. Chem. Soc.* **2007**, 129, 7444.

[46] C. Xu, B. Li, H. Du, F. Kang, Y. Zeng, *J. Power Sources* **2008**, 184, 691.

[47] C. Xu, H. Du, B. Li, F. Kang, Y. Zeng, *J. Electrochem. Soc.* **2009**, 156, A73.

[48] S.-Y. Chung, J. T. Bloking, Y.-M. Chiang, *Nat Mater* **2002**, 1, 123.

[49] Q. Lu, J. G. Chen, J. Q. Xiao, *Angew. Chem. Int. Ed.* **2013**, 52, 1882.

[50] N. N. Greenwood, Earnshaw, A., *Chemistry of the Elements, first ed.*, Pergamon Press, Oxford **1984**.

[51] W. S. Seo, H. H. Jo, K. Lee, B. Kim, S. J. Oh, J. T. Park, *Angewandte Chemie-International Edition* **2004**, 43, 1115.

[52] W. Xiao, H. Xia, J.-Y.-H. Fuh, L. Lu, *J. Electrochem. Soc.* **2009**, 156, A627.

[53] N. J. Tao, *Nat Nano* **2006**, 1, 173.

[54] R. E. Holmlin, R. Haag, M. L. Chabinyc, R. F. Ismagilov, A. E. Cohen, A. Terfort, M. A. Rampi, G. M. Whitesides, *J. Am. Chem. Soc.* **2001**, 123, 5075.

[55] Y. Zhou, F. Jiang, H. Chen, R. Note, H. Mizuseki, Y. Kawazoe, *The Journal of chemical physics* **2008**, 128, 044704.

[56] C. D. Bain, E. B. Troughton, Y. T. Tao, J. Evall, G. M. Whitesides, R. G. Nuzzo, *J. Am. Chem. Soc.* **1989**, 111, 321.

[57] D. L. Allara, R. G. Nuzzo, *Langmuir* **1985**, 1, 52.

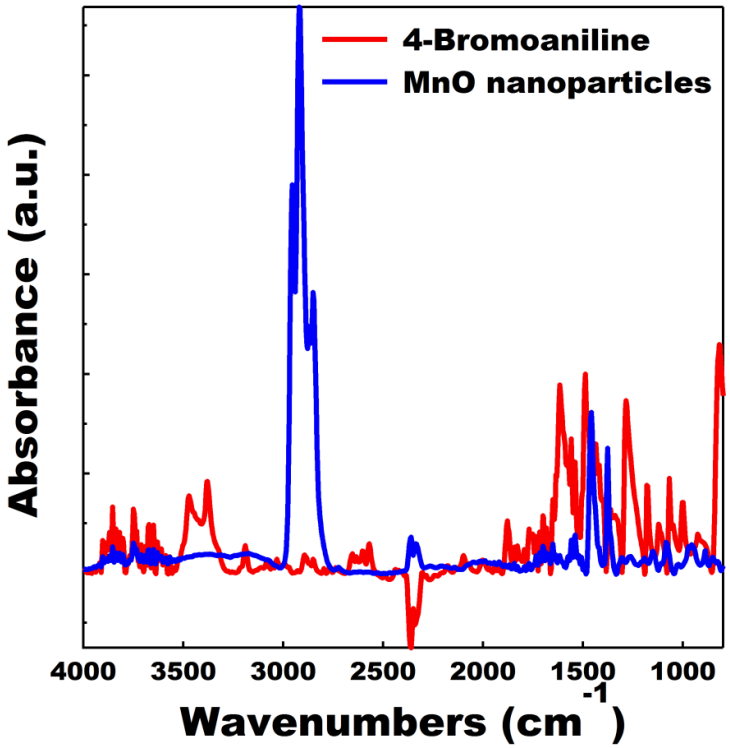

Figure 1. FTIR spectra of MnO nanoparticles synthesized with 4-bromoaniline ligands (blue). The FTIR spectra of neat 4-bromoaniline (red) is provided as a reference.

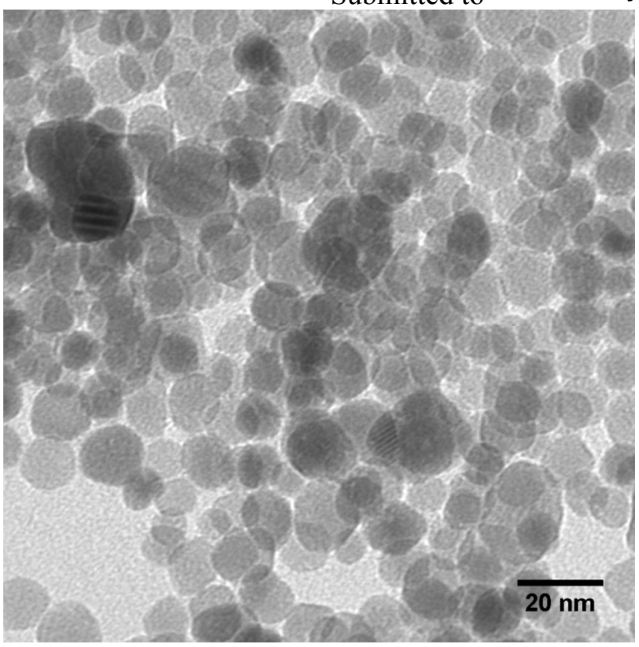

Figure 2. TEM image of MnO nanoparticles synthesized with 4-bromoaniline ligands.

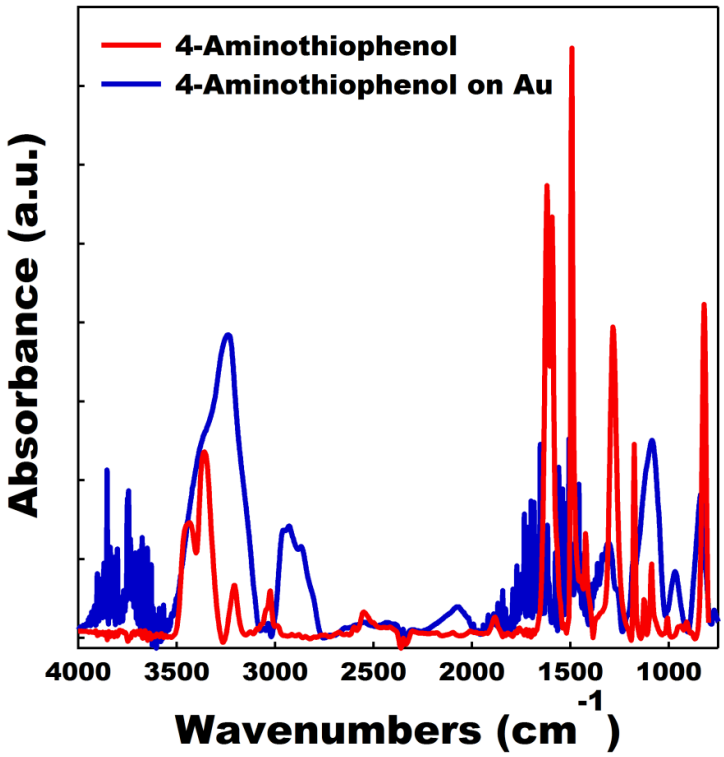

Figure 3. FTIR spectra of 4-aminothiophenol self-assembled monolayer deposited on a gold substrate (blue). The FTIR spectra of neat 4- aminothiophenol (red) is provided as a reference.

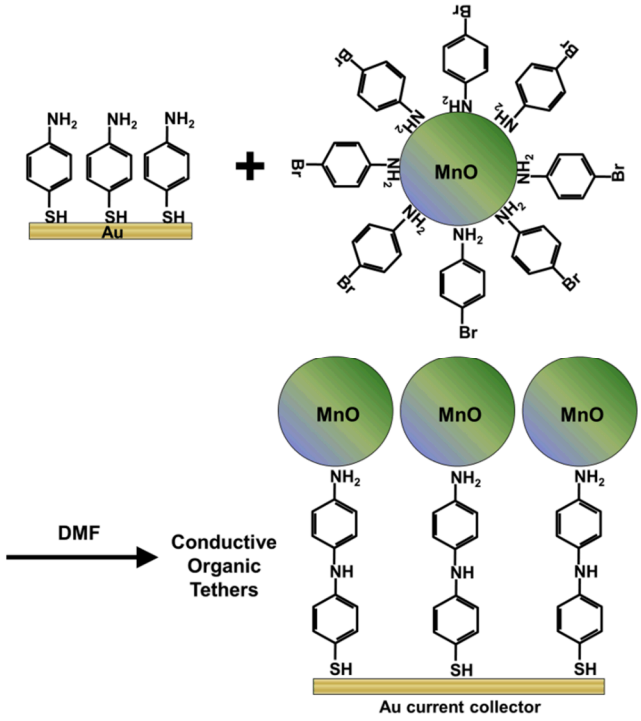

Figure 4. Schematic of the process for reacting a 4-aminothiophenol SAM on gold with 4-bromoaniline functionalized MnO particles to form an array of tethered nanoparticles. After formation of the tethered nanoparticle structure, a largely conductive pathway exists between the MnO nanoparticles and the gold current collector.

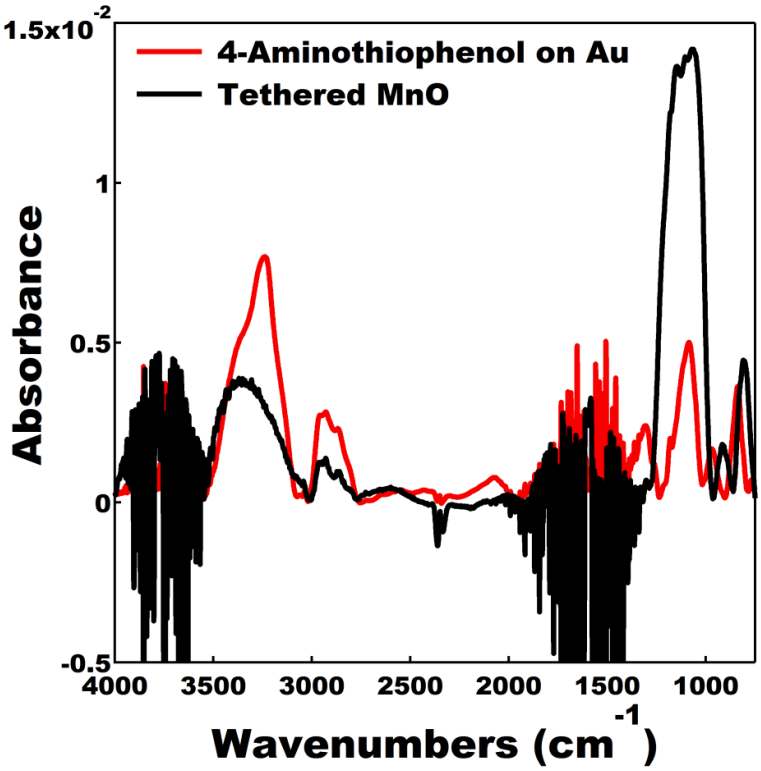

Figure 5. FTIR spectra of an array of MnO nanoparticles bound to a gold substrate via a short conductive organic linkage (black). The FTIR spectra of a 4-aminothiophenol self-assembled monolayer deposited on a gold substrate (red) is provided as a reference.

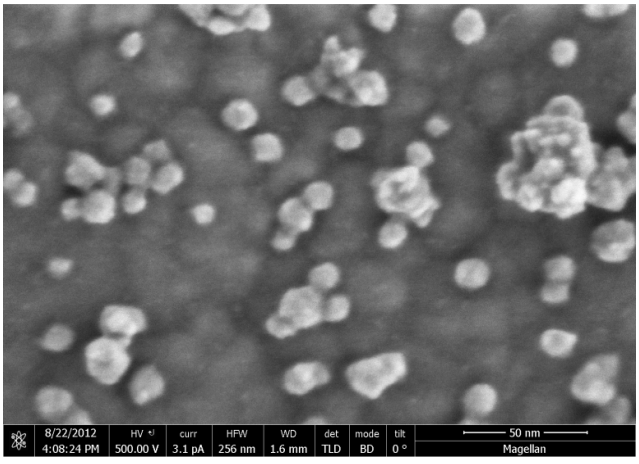

Figure 6. High resolution SEM of array of MnO nanoparticles tethered to a gold surface.

Particle
Submitted to & Particle Systems Characterization

A self-assembled array of MnO nanoparticles is linked to a gold surface using 1.5 nm conducting organic chains. This array creates a new route to oxide supercapacitor electrodes, Li battery electrodes, and catalysts for Li-air batteries and is a step towards addressing many of the challenges currently faced in electrochemical energy storage.

Self-Assembled

T. C. Monson*, T. E. Stevens, C. J. Pearce, C. N. Whitten, R. P. Grant

Self-Assembled Array of Tethered Manganese Oxide Nanoparticles for the Next Generation of Energy Storage

ToC figure ((Please choose one size: 55 mm broad × 50 mm high **or** 110 mm broad × 20 mm high. Please do not use any other dimensions))